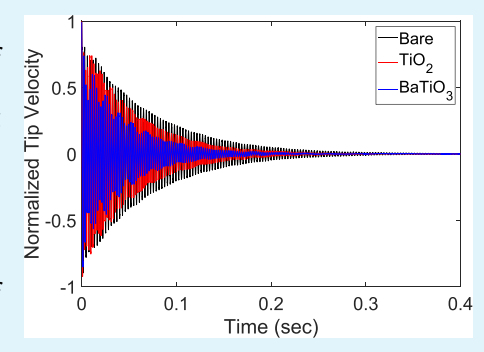


Vibration Damping Mechanism of Fiber-Reinforced Composites with **Integrated Piezoelectric Nanowires**

LoriAnne Groo, [†] Kelsey Steinke, [‡] Daniel J. Inman, [†] and Henry A. Sodano*, [†], [‡]

 † Aerospace Engineering Department and ‡ Materials Science & Engineering Department, University of Michigan, Ann Arbor, Michigan 48109, United States

ABSTRACT: Here, both piezoelectric and nonpiezoelectric nanostructures are used within fiber-reinforced composites to improve the damping capabilities of the host material. This work investigates and isolates the role of both piezoelectricity and the mechanical redistribution of strain on the damping properties of fiber-reinforced composites through the integration of a nanowire interphase between the fiber and matrix. Prior works have successfully studied and reported the effectiveness of modifying the surface of the reinforcing fibers in a composite material using nanowires and other nanostructured interfaces to increase mechanical damping, however, have yet to fully investigate the mechanism dictating the observed behavior. This study analyzes the effects of nonpiezoelectric nanowire interfaces in comparison to piezoelectric nanowire interfaces of the same microscale morphology. The damping properties of carbon



fiber-reinforced composites containing both sets of nanowires are investigated via dynamic mechanical analysis over a range of temperatures as well as modal analysis at the first resonant frequency. The results conclusively indicate that a combination of both mechanical and piezoelectric effects contributes to the significant increase in damping properties of fiber-reinforced composites and quantifies the individual contributions.

KEYWORDS: fiber-reinforced composites, piezoelectric, damping, nanowires, barium titanate, titanium dioxide

INTRODUCTION

Hierarchical nanostructured interfaces within fiber-reinforced composites have previously been shown to benefit multiple mechanical properties. Among the most notable of these benefits are the increased strength and damping of these composites; however, while analysis of the mechanisms dictating the strength has been thoroughly investigated, the origins of the improved damping have remained phenomenological. Initial work investigating the effects of carbon nanotubes (CNTs) on composite damping showed a significant increase in the damping capacity of both polymer composites and fiber-reinforced polymer composites, which was hypothesized to be due to stick-slip behavior and the high levels of friction between the individual nanotubes and the supporting matrix.¹⁻⁷ Ajayan et al. researched the interface between CNTs and the surrounding matrix and the roles of friction and interfacial sliding in the overall damping of the polycarbonate-based composite. It was concluded that the effect of friction and slippage at the nanotube-matrix interface resulted in an increase in loss modulus of over 1000%. This effect, typically referred to as the stick-slip effect, has been well-established as the mechanism dictating the dissipation of energy due to vibration in CNT polymer composites, and knowledge of this underlying mechanism has enabled continued investigation of the damping capabilities of CNT composites. For example, Khan et al. investigated the role of CNTs as a resin reinforcement in carbon fiber prepreg, where the CNT-carbon fiber hybrid composites showed an increase

in damping during free and forced vibration tests due to the stick-slip phenomenon at the interface between the CNTs and supporting matrix. However, although the stick-slip method works effectively to increase damping in the mentioned composites, it should be noted that the mechanism requires poor bonding with the matrix to be effective and is, thus, limited in application.

In addition to carbon nanotubes, zinc oxide (ZnO) nanowires have also been investigated for their use in the dissipation of vibrational energy. Skandani et al. provided a study comparing three sets of composite samples: neat carbon fiber composite samples, samples containing ZnO nanorods grown on the carbon fiber, and composites containing fabric with only part of the full nanorod process completed.8 The results conclusively showed a notable increase in the ratio between the loss modulus and the storage modulus, known as the tan δ , across each of the examined frequencies for the composites with ZnO nanorods compared to the other two composite samples. The authors concluded that the increase in damping properties was primarily due to friction, in a manner similar to CNTs, with an additional partial contribution from the electromechanical coupling of the piezoelectric ZnO nanorods. As the composites containing the piezoelectric nanorods were strained, the energy from the mechanical

Received: September 19, 2019 Accepted: November 22, 2019

Published: November 22, 2019



ACS Applied Materials & Interfaces

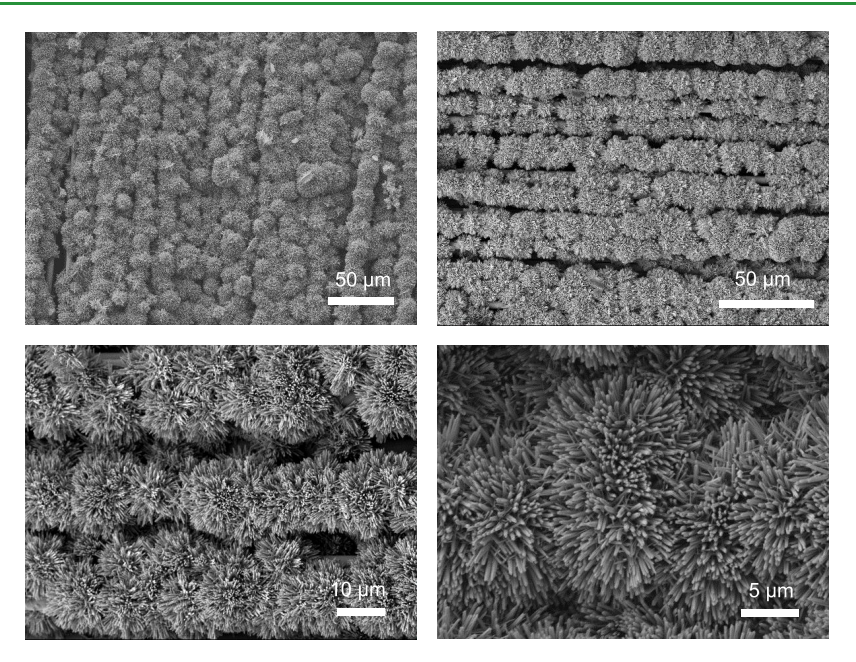


Figure 1. Images of TiO₂ nanowires taken using a scanning electron microscope.

vibration was converted to electrical energy, via the direct piezoelectric effect, and was then dissipated through the conductive pathways formed by the carbon fiber reinforcement. Thus, in this case, the carbon fiber reinforcement served to electrically shunt the generated charge from the nanorods. In addition, Malakooti et al. investigated the relationship between the morphology of conformal ZnO nanowires on the carbon fiber and the energy dissipation or damping of the resulting fiber-reinforced composites.⁹ The work studied three separate aspect ratios of ZnO nanowires and concluded that the lowest aspect ratio provided the greatest benefit with an increased damping of over 200% in $\tan \delta$. However, each sample set showed an increase in damping over neat carbon fiber composites. The increase in damping was attributed to an increase in the volume fraction of the ZnO nanowires, which was found to be largest for the lowest-aspect-ratio nanowires. Similar to CNTs, the overall increase in damping properties was again reasoned to be due to interfacial friction between the nanowires and surrounding matrix as well as mechanical interlocking. It was acknowledged, however, that the piezoelectric nature of the nanowires also contributed to the overall increase in vibration damping by converting the mechanical energy to electrical energy, which was dissipated via the conductive carbon fiber reinforcement. In addition to improving the damping of fiber-reinforced composites, piezoelectric ZnO nanowire interfaces also introduce additional functionality to the material such as energy harvesting and structural health monitoring. 10,11 Notably, these additional functionalities are added without compromising the structural integrity of the fiber, and instead, the ZnO interface has been shown to increase interfacial shear strength and tensile strength of the host composite. 10,12

The combination of the stick-slip mechanism of CNTs with piezoelectric shunt damping to further increase the dissipation of vibrational energy in epoxy-based nanocomposites has been explored by multiple researchers. 13-16 Tian et al. demonstrated the effectiveness of the CNTs in dissipating the electrical energy converted from the dynamic straining of piezoelectric lead zirconate titanate (PZT) nanoparticles. The necessary

amount of CNTs was determined to form conductive pathways to effectively short the circuit formed within the composite, and optimal concentrations of both CNTs and PZT nanoparticles were found in further work. Additionally, this work was expanded by Carponcin et al. to investigate a sandwich configuration with distinct layers of PZT nanoparticles and conductive CNTs, thus further increasing the understanding of the relationship between the piezoelectric PZT nanoparticles and the conductive CNTs. 16 Therefore, a relationship between nonpiezoelectric damping and piezoelectric damping has been established for epoxy-based nanocomposites, but no such relationship has been established for fiber-reinforced composites. ZnO nanowires and piezoelectric PZT nanoparticles in conjunction with CNTs have been shown to increase the damping capabilities in fiberreinforced composites and epoxy-based nanocomposites, respectively, but the role of piezoelectricity versus interfacial friction and mechanical interlocking in dissipating vibrational energy has yet to be fully investigated for fiber-reinforced composites.

This work examines the decoupled role of both mechanical reinforcement and piezoelectricity in dissipating vibrational energy in carbon fiber-reinforced composites. Three sets of samples are studied: neat composites with as-received plainweave carbon fiber, the same carbon fabric with conformal nonpiezoelectric titanium dioxide (TiO2) nanowires, and carbon fiber with piezoelectric barium titanate (BaTiO₃) nanowires with the same microstructure to the previous set. Each sample set is tested using a dynamic mechanical analyzer (DMA) across varying temperatures to determine the loss modulus, storage modulus, and $\tan \delta$. Additionally, a modal analysis of the first resonant frequency of each sample beam using the half-power method is used to validate the conclusions. The materials chosen for this study have a variety of well-documented purposes. Specifically, it is well-known that carbon fiber-reinforced composites are used extensively in several fields including automotive, aircraft, and sporting goods. Additionally, TiO2 is a semiconductor, which has application in photocatalysis, dye-sensitized solar cells, and the

ACS Applied Materials & Interfaces

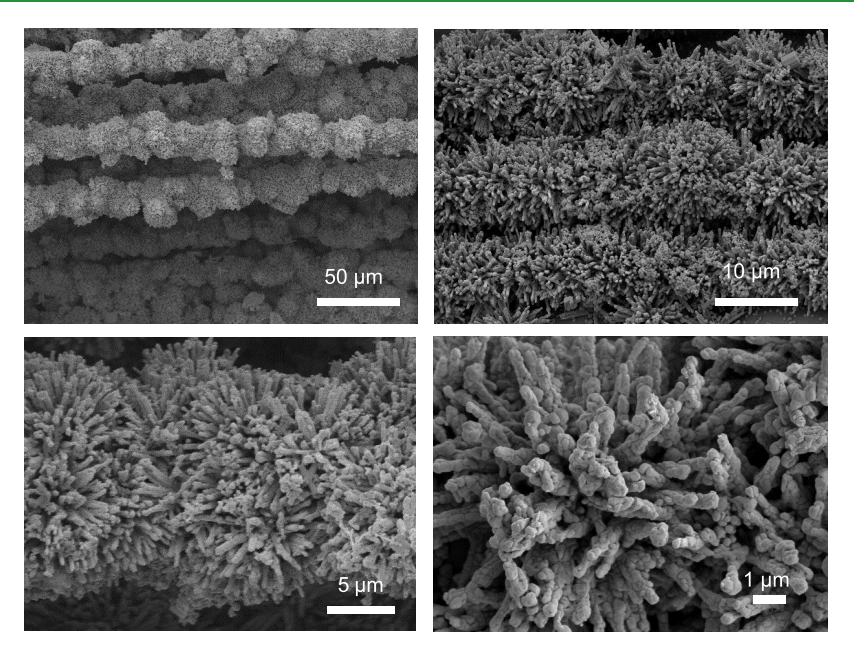


Figure 2. Images of BaTiO₃ nanowires taken using a scanning electron microscope.

electrochemical splitting of water among others. ^{17–19} Furthermore, ferroelectric BaTiO₃ also has multiple applications such as energy harvesting and flow sensing. ²⁰ However, the driving purpose of this paper is to scientifically investigate the general benefit of piezoelectric nanowires over nonpiezoelectric nanowires for damping. Since the BaTiO₃ nanowires are synthesized using TiO₂ nanowires as a template, the microstructure remains unchanged during the conversion to ferroelectric nanowires. Thus, this combination of materials enables the separation of the damping due to the ferroelectric nature of the nanowires from the majority of the contributions due to mechanical damping, which has not yet been done for fiber-reinforced composites.

MATERIALS AND METHODS

TiO₂ Synthesis. TiO₂ nanowires were grown directly onto the carbon fiber using a two-step process. Initially, the plain-weave carbon fabric (Hexcel HexForce Style SGP196-P, 5.80 oz/yd2) was cleaned in sequential washes of boiling acetone, isopropanol, and deionized (DI) water to remove organic contaminants from the fiber surface. The fabric was boiled in each solvent for 15 min, after which it was dried thoroughly in a convection oven set at 100 °C. After the fabric was thoroughly dried, it was dipped in a TiO2 sol-gel solution using a process outlined by Bowland et al. 20-22 The solution was made by mixing 17 mL of isopropanol (Fisher Chemical, Certified ACS) and 0.04 mL of 33% hydrochloric acid (Fisher Chemical, Certified ACS) with 1.25 mL of titanium isopropoxide (Alfa Aesar, 97+%). After being dipped in the solution, the fabric was annealed at 120 °C for 2 h. The annealing step was followed by TiO2 nanowire growth using a hydrothermal reaction consisting of 40 mL of DI water combined with 40 mL of 33% hydrochloric acid (Fisher Chemical, Certified ACS). 23-25 After the water and acid were allowed to thoroughly mix, 5 g of titanium(IV) chloride (Alfa Aesar, 99.0% min) was added dropwise while constantly stirring the solution. Previous work has shown that using titanium chloride as the titanium source results in a uniform nanowire layer with the least amount of cauliflower-type growth, which is commonly seen from the hydrothermal TiO2 nanowire growth process on the carbon fiber. 23 The fabric and growth solution were placed in a stainless steel reactor with a poly(tetrafluoroethylene) (PTFE) liner, sealed, and subsequently placed in a convection oven at 170 °C for 7 h before allowing it to slowly cool down to room temperature. After the solution had fully

cooled, the fabric with ${\rm TiO_2}$ nanowires was rinsed thoroughly with DI water and dried for several hours in a convection oven. Finally, the nanowires were examined using a scanning electron microscope (SEM) (JSM-7800F). Representative images of the ${\rm TiO_2}$ nanowires on the carbon fiber surface are shown in Figure 1.

BaTiO₃ Synthesis. The TiO₂ nanowires were then used as templates for the formation of BaTiO₃ by the diffusion of barium ions into the TiO2 structure while preserving the microscale morphology of the nanowires. The resulting nanowires have a similar microstructure as the TiO₂ nanowires, however, have ferroelectric coupling. To accomplish this, the TiO₂ nanowire-coated carbon fiber was thoroughly rinsed and dried before being placed into a second hydrothermal reaction for the conversion to BaTiO₃ nanowires.²⁴ The solution was prepared by boiling 80 mL of DI water and then adding 2.056 g (0.15 M) of barium hydroxide [Ba(OH)₂] to the boiling DI water to act as the barium source for the conversion. The solution and carbon fabric coated with TiO2 nanowires were then placed in a PTFE-lined steel reactor and immediately sealed and placed in a convection oven at 210 °C for 24 h. The second hydrothermal reaction serves to hydrolyze the surface of the TiO₂ nanowires, which leads to a dissolution reprecipitation process that drives the diffusion of the barium ions into the TiO₂ structure resulting in BaTiO₃ nanowires.²⁷⁻³⁰ As before, the reactor and solution were allowed to cool slowly to room temperature. The fabric was then thoroughly rinsed with DI water, after which it was dipped into a solution of roughly 500 mL of DI water with approximately 0.5 mL of 33% hydrochloric acid (Fisher Chemical, Certified ACS) to neutralize the high pH of the reaction solution. The fabric with BaTiO₃ nanowires was characterized using SEM, which can be seen in Figure 2. As is shown in the figure, the nanowires maintain the same microstructure through the conversion process; however, the surface texture of the nanowires on a nanoscale is slightly changed as a result of the reprecipitation process, which results in a polycrystalline shell surrounding a single-crystal nanowire.

In addition to analysis using SEM images, the composition of the TiO_2 and $BaTiO_3$ nanowires was both evaluated using X-ray diffraction (XRD). The rutile TiO_2 nanowires show signature peaks at approximately 27, 36, and 55°, while the $BaTiO_3$ nanowires show dominant peaks at 32, 39, and 45°, as predicted from the Joint Committee on Powder Diffraction Standards (JCPDS) Card No. 65-0190 and 05-0626, respectively. 20,31 It should be noted that the $BaTiO_3$ nanowires do show small peaks at 27, 36, and 55° corresponding to TiO_2 due to the fact that the conversion is less than 100%; however, the conversion rate results in piezoelectric

nanowires as shown in the previous work and was, thus, considered sufficient for the purpose of this study. 20,25 The resulting XRD spectra are shown in Figure 3.

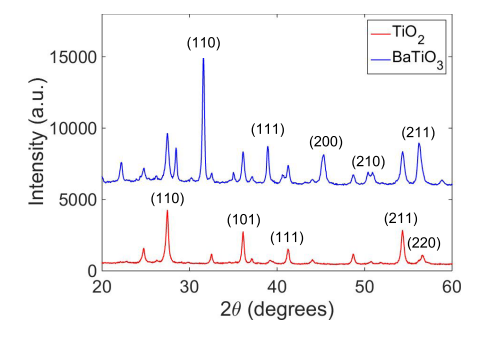


Figure 3. XRD spectra of TiO2 and BaTiO3 nanowires.

Composite Fabrication. Following the completion of the nanowire growth and conversion, the three sets of composite samples were fabricated using the same composite layup process. Six plies of the neat carbon fiber, carbon fiber with TiO₂ nanowires, and carbon fiber with BaTiO3 nanowires were laid up separately using a hand layup process with EPONTM resin 862 (received from Miller Stephenson) and EPIKURETM curing agent 3230 (received from Hexion) in a 100:35 ratio, respectively. Each composite was then kept under vacuum and placed in a hot press initially at room temperature under a pressure of 100 psi. After 10 h at room temperature, the temperature was increased to 80 °C for 2 h followed by a 3 h postcure at 125 °C. After completion of the composite layup process, the fabricated panels were then cut into 60 mm long and 10 mm wide beams for testing. Due to the addition of the nanowire interface in the samples with TiO2 and BaTiO3, the thickness of the nanowire composites was higher than that of the neat composite samples. Specifically, the samples with TiO2 nanowires had an average thickness of 1.27 mm, and those with integrated BaTiO₃ nanowires had an average thickness of 1.45 mm, while neat carbon fiber composites had an average thickness of only 1.05 mm. However, it should be noted that the nanowire interface is located only on the fabric surface exposed during the hydrothermal reaction. As a result, the nanowires are not distributed through the thickness of each tow or ply and are localized only to the interface between plies. The resulting

areal weights of the fabric are approximately 197, 301, and 321 g/m² for the bare fabric, fabric coated with TiO2 nanowires, and fabric coated with BaTiO₃ nanowires, respectively. SEM images of the crosssection of the completed composite showing the preserved nanowire structure can be seen in Figure 4. Note that the nanowires are not perfectly uniform; however, the nanowire structures seen in Figures 1 and 2 are not altered through the layup process.

To further analyze the resulting composites, thermogravimetric analysis (TGA) using a SDT Q600 was used to determine the weight fractions of the epoxy, fibers, and nanowire interface for three samples of each composite sample set, nine samples in total. Each sample was heated at a rate of 5 °C/min from room temperature to 1000 °C. The sample was then held at 1000 °C for 1 h to fully remove the carbon fiber. The measured density of the composites in combination with the density of the epoxy and fibers as provided by the manufacturers was then used to calculate the approximate volume fraction of each component of the composite. The resulting volume percent of each component is shown in Table 1 for reference. From the table, the fiber

Table 1. Volume Fractions of Fibers, Matrix, and Nanowires for Each Sample Set

sample set	fiber volume fraction (%)	matrix volume fraction (%)	nanowire volume fraction (%)
neat carbon fiber	73	27	
carbon fiber with ${\rm TiO_2}$	61	30	9
carbon fiber with $BaTiO_3$	58	31	11

volume fraction of the bare samples is the highest at 73%, and the fiber volume fractions of the TiO2 and BaTiO3 samples are 61 and 58%, respectively. It is also critical to note that the volume fraction of the matrix in the TiO₂ and BaTiO₃ samples is within 1%. Thus, additional epoxy is not responsible for the change in damping between the two sample sets containing nanowires.

■ RESULTS AND DISCUSSION

Dynamic Mechanical Analysis. Dynamic mechanical analysis has been well-established as an investigative method for the damping properties of fiber-reinforced composites.³² Specifically, the testing procedure in this work followed that

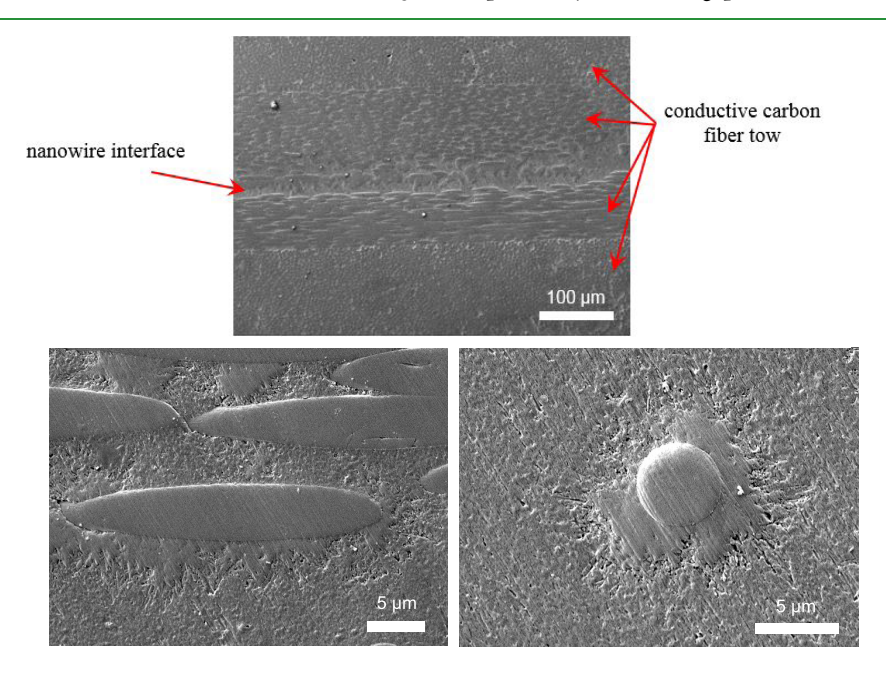


Figure 4. SEM images of portions of the composite cross-section showing the BaTiO₃ nanowires adhered to the individual fibers.

described by Malakooti et al.9 A TA Instruments DMA Q800 was used to perform these tests with the dual cantilever clamp attachment, and the average thickness and width were measured for each sample. A loading frequency of 50 Hz was used while the specimens were heated at a ramp rate of 2 °C/min from room temperature up to 120 °C. An image of the test setup can be seen in Figure 5.



Figure 5. Image of the DMA testing setup with a representative sample.

A minimum of four samples was tested for each sample set, the results of which were averaged for each set. The resulting averaged curves from the DMA, shown in Figure 6a, indicate a decrease in the storage modulus (E') of both sets of nanowire

composites when compared to neat carbon fiber composites. This is due to a combination of the decreased fiber volume fraction in the nanowire samples and an increase in the thickness of the samples when nanowires are grown onto the fiber surfaces. As previously stated, the composites with integrated TiO2 nanowires had an average thickness of 1.27 mm, and those with integrated BaTiO3 nanowires had an average thickness of 1.45 mm, versus the neat composite samples with a thickness of 1.05 mm. Because the nanowires are adhered to the fabric itself, there is an imposed physical limitation on the fiber volume fraction due to the additional space created for the supporting matrix, thus leading to a slight decrease in the fiber volume fraction of the nanowire composites studied in this work. For the investigative purposes of this study, $\tan \delta$ was considered the primary figure of merit, since it correlates to the damping capacity of the material, which is the focus of this work. Thus, the damping of each composite is evaluated by examining the ratio between the measured loss modulus (E'') and the storage modulus (E'), which is shown in Figure 6c as $\tan \delta$, over the full temperature range analyzed. The figure clearly shows an increase in $\tan \delta$ from the averaged bare samples, to the nonpiezoelectric TiO2 nanowire composite, to the ferroelectric BaTiO₃ nanowire composite.

For a clearer analysis of the trends in the damping response of the sample sets, the increase in $\tan \delta$ of the nanowire composites normalized by the baseline value of $\tan \delta$ from the neat composite sample is shown in Figure 7. Both $\tan \delta$ at ambient temperature (Figure 7a) and the peak value of tan δ occurring at the glass transition temperature (Figure 7b) were considered. From the figure, it is clear that the nonpiezoelectric TiO₂ nanowires contribute to a significant increase in the damping properties of the host composite. While this increase is still visible at room temperature, the increase is most significant at the glass transition temperature where the tan δ peaks. This is due to the increased strain resulting from the

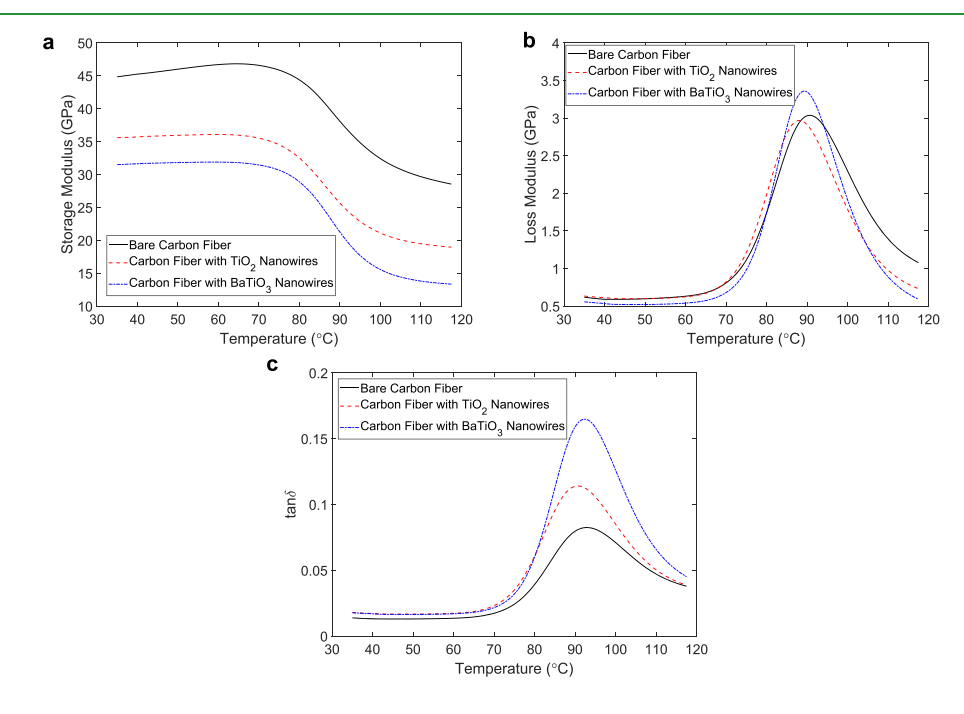


Figure 6. Averaged (a) storage modulus (E'), (b) loss modulus (E''), and (c) $\tan \delta$ of the bare carbon fiber, carbon fiber with TiO_{2} , and carbon fiber with BaTiO3 composite samples.

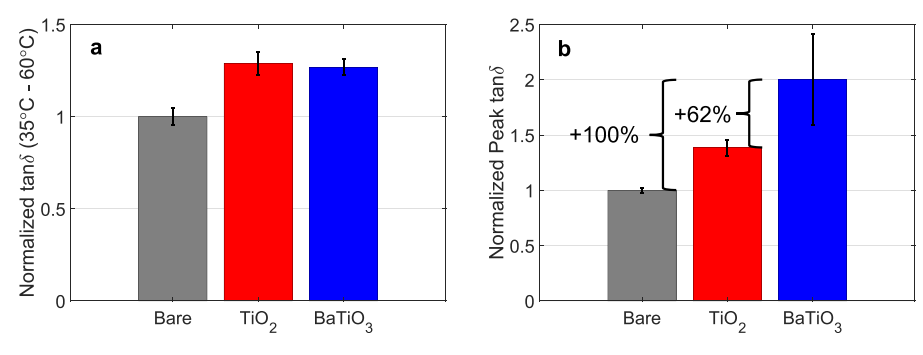


Figure 7. (a) Normalized tan δ at the operating temperature and (b) normalized tan δ at the transition temperature.

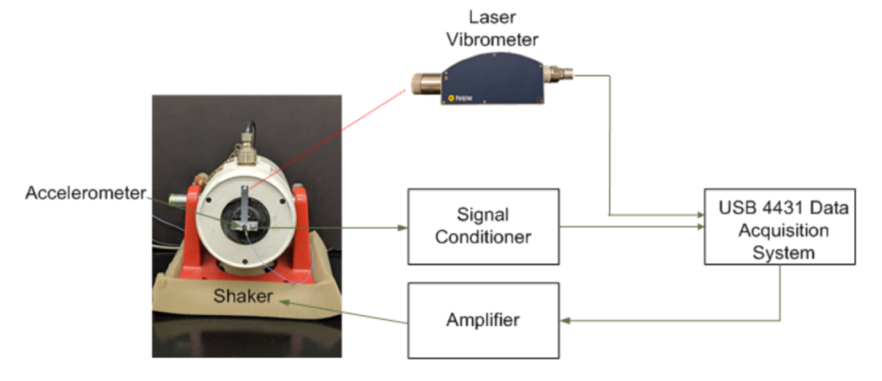


Figure 8. Schematic of the test setup for modal analysis.

softening of the composite at elevated temperatures around the transition temperature of the epoxy matrix. This also results in an increased variation in results due to the large magnitude of the strain and imposed damping of the nanowires in these conditions. Rather than an abrupt and discontinuous transition from the fiber to matrix as is typically seen in traditional fiberreinforced composites, the nanowires grown directly onto the reinforcing fibers form an interphase between the reinforcing fibers and matrix, which creates a bridge between each constituent, resulting in a modulus gradient and, thus, a more continuous transition in load between the fiber and matrix. This, thus, leads to a more optimal strain transfer and efficient energy dissipation.³⁶ The enhanced damping properties of the TiO₂ nanowires are attributed to the transition of the interfacial shear stress that occurs during bending to the polymer matrix, which has higher damping than the interface. Malakooti et al. used digital image correlation (DIC) to characterize the strain distribution across a functionally graded nanowire interface and showed that the presence of the stiff nanowires causes limited shear strain in the interphase and high strain in the polymer.²⁹ The deflection of the shear strain away from the interface and into the polymer is responsible for the previously observed improvement in interfacial shear strength and would also increase damping. Based on both the referenced DIC analysis and the measurements made here, it can be concluded that the presence of the nanowires increases damping through a modification of the stress location and is a result of the functionally graded interface.

The conversion of the TiO₂ nanowires to BaTiO₃ maintains the microscale morphology of the interface, however, incorporates ferroelectricity into the composite and, therefore, provides a means to separate the damping resulting from mechanical and piezoelectric effects. As can be seen in Figure 8a, the difference between the damping of the samples with

TiO₂ nanowires compared to those with BaTiO₃ nanowires at room temperature is negligible. This is due to the low magnitude strain, which is experienced by the samples at room temperature and low frequency since the energy dissipation through joule heating is proportional to strain as it is a direct result of the piezoelectric effect. In contrast, Figure 8b shows that at the T_{o} , the ferroelectric BaTiO₃ nanowires show a 100% increase in damping over neat composites and 62% over those with TiO2 nanowires. This can be attributed to the ferroelectric properties of the BaTiO3 nanowires, which leads to increased energy dissipation through the conversion of vibrational energy to electrical energy. The physical vibration of the composite sample results in a charge generation, which is immediately dissipated as the composite is fabricated from electrically conductive carbon fibers. This mechanism of energy dissipation is the same as that seen in piezoelectricreinforced metal matrix composites, which take advantage of the conductive metal matrix to dissipate energy via joule heating; however, in this work, the fiber reinforcement serves as the conductive material rather than the matrix.37-However, it should be noted that the surface texture of the BaTiO₃ nanowires on the nanoscale is slightly altered from that of the TiO2 nanowires, which may result in a slight increase in mechanical damping, yet this difference is not considered significant enough to contribute an increase of ~62% in the damping, as is detected using the $\tan\delta$ measurements.

Modal Analysis. To further confirm the results obtained using the DMA, modal analysis tests were completed to determine the damping properties using the well-established "half-power" method. ^{40,41} In short, each sample beam was excited using an LDS V406 electromagnetic shaker driven with a Gaussian white noise signal generated using a NI 4431 data acquisition system (DAQ) connected to a Labworks Inc. PA-119 power amplifier. The resulting tip velocity was recorded using a Polytec OFV-5000 laser vibrometer system, and the base acceleration of the sample was simultaneously measured using a PCB 352C22 accelerometer, which was connected to a PCB model 482A16 ICP signal conditioner. The resulting power spectrum was then calculated over the frequency range of interest using the built-in frequency response function (FRF) in LabVIEW Signal Express. A schematic of the test setup is shown in Figure 8.

To calculate the damping ratio for each sample, the frequency response at the first natural frequency was examined. The frequency corresponding to the peak magnitude (natural frequency) and the frequency of the two half-power points (3 dB decrease from the peak value) on either side of the peak level were analyzed to determine the damping ratio. Each of these points is shown on a representative frequency response in Figure 9. The damping ratio, ζ , can then be calculated as the difference between the two half-power frequencies, $\Delta \omega$, divided by twice the natural frequency, ω_n , as follows

$$\zeta = \frac{\omega_2 - \omega_1}{2\omega_n} \tag{1}$$

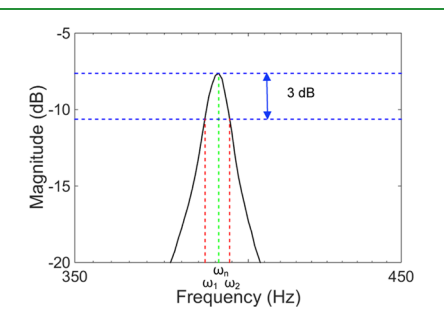


Figure 9. Modal analysis of the first natural frequency.

Upon visual inspection of the first natural frequency of one representative sample from each set shown in Figure 10a, it can be seen that the bare sample, which demonstrates the least amount of quantitative damping, shows the sharpest peak with a broader and lower peak seen from each of the nanowire samples. The averaged damping ratios are compared in Figure 10b, while the damping ratios normalized by the neat composite values are compared in Figure 10c. It can be observed in both figures that the same trends identified from the DMA testing can also be observed using model analysis. Furthermore, the results from the modal analysis at the first natural frequency more closely align with those observed from the normalized $\tan\delta$ at the glass transition temperature from DMA testing. This similarity in trend is due to the increased motion of the composite beams both at the transition temperature and the resonant frequency. The nonpiezoelectric TiO₂ nanowires were found to have a broader peak at the natural frequency, and thus displaying a 60% increase in the damping ratio over the neat composite sample. As previously discussed, this is attributed to the mechanical interlocking and redistribution of shear strain within the composite resulting from the nanowire interphase between the reinforcing fibers and the polymer matrix. Additionally, the ferroelectric BaTiO₃ nanowires showed further broadening of the peak due to additional damping in the composite as represented by a 110% increase in the damping ratio over the neat composite sample and 50% increase in the damping ratio over the TiO₂ nanowire sample. This is attributed to the dissipation of energy via conversion to electrical energy by the nanowires, which is then effectively dissipated through joule heating of the carbon fiber reinforcements. This electromechanical effect works in addition to the same mechanical effects displayed by the TiO₂ nanowires.

In addition to the half-power method, the log-decrement method is also frequently used for damping analysis. 42 In short,

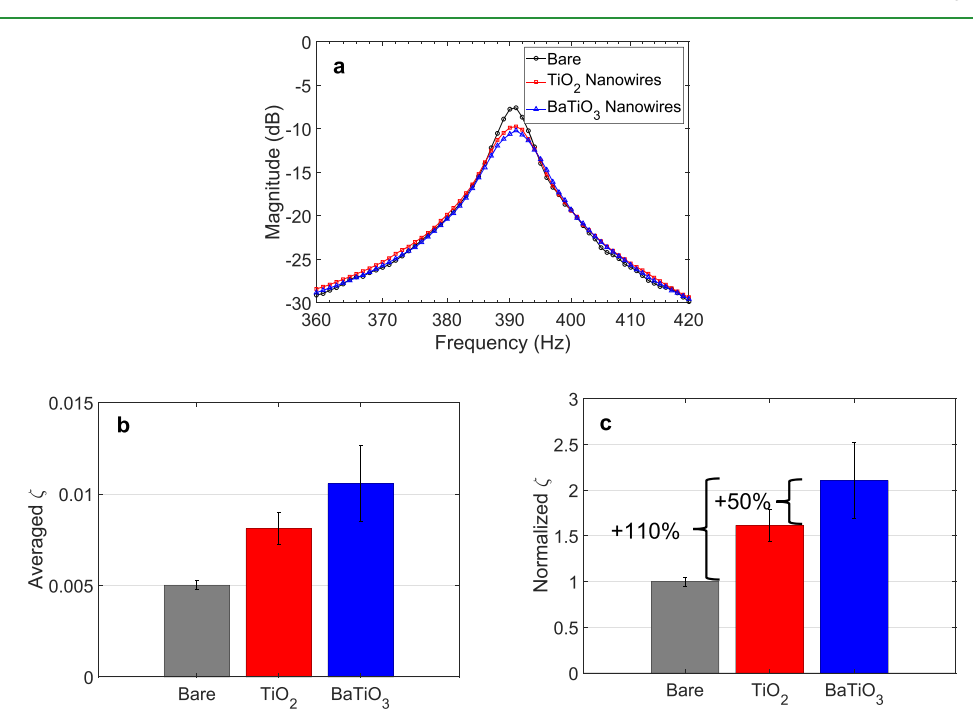


Figure 10. (a) Representative frequency response of bare carbon fiber sample, carbon fiber with TiO₂ nanowires, and carbon fiber with BaTiO₃ nanowires. (b) Averaged ζ and (c) normalized ζ for bare carbon fiber, carbon fiber with TiO₂, and carbon fiber with BaTiO₃ composite samples.

the log-decrement method analyzes the amount of time required for the decay of physical vibratory oscillations following an impulse. A specimen with higher damping will more efficiently dissipate energy leading to a faster decay in the magnitude of the vibratory response when compared to a specimen with lower damping, and thus approaching the steady state at a quicker rate. Therefore, to further confirm the increased damping of the composite specimen sets, each composite beam used for both the dynamic mechanical analysis and the half-power method was excited with an impulse, while the tip velocity was measured using the same laser vibrometer and data acquisition system as was used for the half-power method. To more clearly visualize the difference in the rate of decay, the tip velocity of each sample was normalized by the maximum magnitude to have a normalized maximum value of one for each sample. An analysis of the resulting normalized responses, shown in Figure 11, shows that

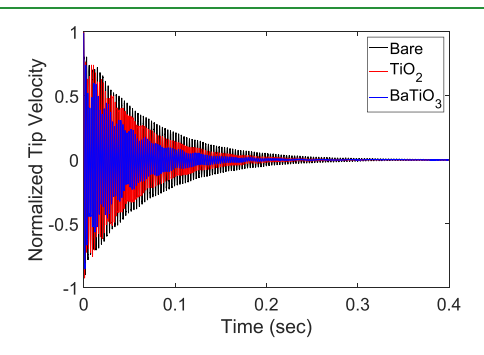


Figure 11. Time response of the sample tip velocity resulting from an impulse of bare, TiO2, and BaTiO3 samples.

the BaTiO₃ sample dissipates vibrational energy most rapidly followed by the TiO2 sample, while the bare sample shows the longest time required to reach the steady state. Therefore, by visual inspection, the damping trend clearly follows that observed using dynamic mechanical analysis and the halfpower method without the need for further analysis of the response.

CONCLUSIONS

This work establishes the role of piezoelectricity versus purely mechanical effects on damping of carbon fiber-reinforced composites containing ferroelectric nanostructures. To accomplish this, three sets of samples were tested: baseline composite samples fabricated using as-received plain-weave carbon fabric, composite samples with TiO2 nanowires, and ferroelectric BaTiO₃ nanowires. Each sample set was evaluated using two methods: DMA analysis and the half-power method. The results from both sets of independent tests show a substantial increase in damping properties from the baseline samples to the nonferroelectric TiO2 nanowire samples, which is attributed to the mechanical interlocking of the nanowires with the polymer matrix and the formation of greater shear stress in the dissipative polymer matrix rather than the interface. The influence of piezoelectric coupling on the damping behavior of the composite was quantified through the transformation of the TiO₂ nanowires to ferroelectric BaTiO₃ nanowires without changing the microstructure and, thus, without significantly changing the mechanical contribution of the interphase to damping. Following conversion to a ferroelectric structure, the damping was minimally affected at

low strain magnitudes such as are experienced at room temperature and low frequency; however, the damping further increased by 100-110% over nonferroelectric TiO2 and 50-62% over the neat composite as measured at high strains, i.e., dynamic mechanical analysis at the T_g and modal analysis of the first natural frequency. The additional increase in damping can be attributed to the piezoelectric behavior, which converts the vibrational energy to electrical energy that is dissipated through joule heating due to the conductive carbon fibers. It can, thus, be concluded that the addition of piezoelectric nanostructures provides a significant and nearly equal contribution as the mechanical effects of nonpiezoelectric nanostructures in carbon fiber-reinforced composites.

AUTHOR INFORMATION

Corresponding Author

*E-mail: hsodano@umich.edu.

ORCID ®

LoriAnne Groo: 0000-0001-5296-1354 Henry A. Sodano: 0000-0001-6269-1802

The authors declare no competing financial interest.

ACKNOWLEDGMENTS

This work was supported by the National Science Foundation Graduate Research Fellowship Program, the Army Research Office under Contract # W911NF-16-1-0229, National Science Foundation under Grant # CMMI-1762369, and in part by the University of Michigan.

REFERENCES

- (1) Ajayan, P. M.; Suhr, J.; Koratkar, N. Utilizing Interfaces in Carbon Nanotube Reinforced Polymer Composites for Structural Damping. J. Mater. Sci. 2006, 41, 7824-7829.
- (2) Khan, S. U.; Li, C. Y.; Siddiqui, N. A.; Kim, J.-K. Vibration Damping Characteristics of Carbon Fiber-Reinforced Composites Containing Multi-Walled Carbon Nanotubes. Compos. Sci. Technol. 2011, 71, 1486-1494.
- (3) Zhou, X.; Shin, E.; Wang, K. W.; Bakis, C. E. Interfacial Damping Characteristics of Carbon Nanotube-Based Composites. Compos. Sci. Technol. 2004, 64, 2425-2437.
- (4) Gibson, R. F.; Ayorinde, E. O.; Wen, Y.-F. Vibrations of Carbon Nanotubes and Their Composites: A Review. Compos. Sci. Technol. **2007**, *67*, 1–28.
- (5) Ci, L.; Suhr, J.; Pushparaj, V.; Zhang, X.; Ajayan, P. M. Continuous Carbon Nanotube Reinforced Composites. Nano Lett. 2008, 8, 2762-2766.
- (6) Koratkar, N.; Wei, B.; Ajayan, P. M. Carbon Nanotube Films for Damping Applications. Adv. Mater. 2002, 14, 997-1000.
- (7) Koratkar, N. A.; Wei, B.; Ajayan, P. M. Multifunctional Structural Reinforcement Featuring Carbon Nanotube Films. Compos. Sci. Technol. 2003, 63, 1525-1531.
- (8) Skandani, A. A.; Masghouni, N.; Case, S. W.; Leo, D. J.; Al-Haik, M. Enhanced Vibration Damping of Carbon Fibers-ZnO Nanorods Hybrid Composites. Appl. Phys. Lett. 2012, 101, No. 073111.
- (9) Malakooti, M. H.; Hwang, H.-S.; Sodano, H. A. Morphology-Controlled ZnO Nanowire Arrays for Tailored Hybrid Composites with High Damping. ACS Appl. Mater. Interfaces 2015, 7, 332-339.
- (10) Malakooti, M. H.; Patterson, B. A.; Hwang, H.-S.; Sodano, H. A. ZnO Nanowire Interfaces for High Strength Multifunctional Composites with Embedded Energy Harvesting. Energy Environ. Sci. 2016, 9, 634-643.
- (11) Groo, L.; Inman, D. J.; Sodano, H. A. In Situ Damage Detection for Fiber-Reinforced Composites Using Integrated Zinc Oxide Nanowires. Adv. Funct. Mater. 2018, 28, No. 1802846.

- (12) Ehlert, G. J.; Sodano, H. A. Zinc Oxide Nanowire Interphase for Enhanced Interfacial Strength in Lightweight Polymer Fiber Composites. ACS Appl. Mater. Interfaces 2009, 1, 1827–1833.
- (13) Tian, S.; Cui, F.; Wang, X. New Type of Piezo-Damping Epoxy-Matrix Composites with Multi-Walled Carbon Nanotubes and Lead Zirconate Titanate. *Mater. Lett.* **2008**, *62*, 3859–3861.
- (14) Tian, S.; Wang, X. Fabrication and Performances of Epoxy/Multi-Walled Carbon Nanotubes/Piezoelectric Ceramic Composites as Rigid Piezo-Damping Materials. *J. Mater. Sci.* **2008**, *43*, 4979–4987.
- (15) Ma, M.; Wang, X. Preparation, Microstructure and Properties of Epoxy-Based Composites Containing Carbon Nanotubes and PMN-PZT Piezoceramics as Rigid Piezo-Damping Materials. *Mater. Chem. Phys.* **2009**, *116*, 191–197.
- (16) Carponcin, D.; Dantras, E.; Michon, G.; Dandurand, J.; Aridon, G.; Levallois, F.; Cadiergues, L.; Lacabanne, C. New Hybrid Polymer Nanocomposites for Passive Vibration Damping by Incorporation of Carbon Nanotubes and Lead Zirconate Titanate Particles. *J. Non-Cryst. Solids* **2015**, 409, 20–26.
- (17) Asahi, R.; Morikawa, T.; Ohwaki, T.; Aoki, K.; Taga, Y. Visible-Light Photocatalysis in Nitrogen-Doped Titanium Oxides. *Science* **2001**, 293, 269.
- (18) Boercker, J.; Enache-Pommer, E.; Aydil, E. Growth Mechanism of Titanium Dioxide Nanowires for Dye-Sensitized Solar Cells. *Nanotechnology* **2008**, *19*, No. 095604.
- (19) Fujishima, A.; Honda, K. Electrochemical Photolysis of Water at a Semiconductor Electrode. *Nature* **1972**, 238, 37–38.
- (20) Bowland, C.; Zhou, Z.; Sodano, H. A. Multifunctional Barium Titanate Coated Carbon Fibers. *Adv. Funct. Mater.* **2014**, 24, 6303–6308.
- (21) Bowland, C. C.; Malakooti, M. H.; Zhou, Z.; Sodano, H. A. Highly Aligned Arrays of High Aspect Ratio Barium Titanate Nanowires via Hydrothermal Synthesis. *Appl. Phys. Lett.* **2015**, *106*, No. 222903
- (22) Bowland, C. C. Conformal Growth Method of Ferroelectric Materials for Multifunctional Composites. Ph.D. Thesis, University of Florida: Gainesville, FL, 2016.
- (23) Khan, M. A. Development of TiO₂ Nanowires on Carbon Fiber Substrate Utilizing Different Titanium Precursors, Proceedings of the 2nd Southwest Energy Science and Engineering Symposium, March 24, 2012; University of Texas El Paso: El Paso, TX, 2012.
- (24) Zhou, Z.; Tang, H.; Sodano, H. A. Vertically Aligned Arrays of BaTiO₃ Nanowires. ACS Appl. Mater. Interfaces **2013**, 5, 11894–11899.
- (25) Zhou, Z.; Bowland, C. C.; Patterson, B. A.; Malakooti, M. H.; Sodano, H. A. Conformal BaTiO3 Films with High Piezoelectric Coupling Through an Optimized Hydrothermal Synthesis. *ACS Appl. Mater. Interfaces* **2016**, *8*, 21446–21453.
- (26) Koka, A.; Zhou, Z.; Sodano, H. A. Vertically Aligned BaTiO₃ Nanowire Arrays for Energy Harvesting. *Energy Environ. Sci.* **2014**, *7*, 288–296.
- (27) Hertl, W. Kinetics of Barium Titanate Synthesis. *J. Am. Ceram. Soc.* **1988**, *71*, 879–883.
- (28) Bacsa, R.; Ravindranathan, P.; Dougherty, J. Electrochemical, Hydrothermal, and Electrochemical-Hydrothermal Synthesis of Barium Titanate Thin Films on Titanium Substrates. *J. Mater. Res.* **1992**, *7*, 423–428.
- (29) Yoshimura, M.; Yoo, S.-E.; Hayashi, M.; Ishizawa, N. Preparation of BaTiO3 Thin Film by Hydrothermal Electrochemical Method. *Jpn. J. Appl. Phys.* **1989**, 28, L2007–L2009.
- (30) Ciftci, E.; Rahaman, M.; Shumsky, M. Hydrothermal Precipitation and Characterization of Nanocrystalline BaTiO₃ Particles. *J. Mater. Sci.* **2001**, *36*, 4875–4882.
- (31) Thamaphat, K.; Limsuwan, P.; Ngotawornchai, B. Phase Characterization of TiO₂ Powder by XRD and TEM. *Kasetsart J.: Nat. Sci.* **2008**, *42*, 357–361.
- (32) Mohanty, S.; Verma, S. K.; Nayak, S. K. Dynamic Mechanical and Thermal Properties of MAPE Treated Jute/HDPE Composites. *Compos. Sci. Technol.* **2006**, *66*, 538–547.

- (33) Idicula, M.; Malhotra, S.; Joseph, K.; Thomas, S. Dynamic Mechanical Analysis of Randomly Oriented Intimately Mixed Short Banana/Sisal Hybrid Fibre Reinforced Polyester Composites. *Compos. Sci. Technol.* **2005**, *65*, 1077–1087.
- (34) Dalmas, F.; Cavaillé, J.-Y.; Gauthier, C.; Chazeau, L.; Dendievel, R. Viscoelastic Behavior and Electrical Properties of Flexible Nanofiber Filled Polymer Nanocomposites. Influence of Processing Conditions. *Compos. Sci. Technol.* **2007**, *67*, 829–839.
- (35) Gibson, R. F. Vibration-Test Methods for Dynamic-Mechanical-Property Characterization. In *Manual on Experimental Methods for Mechanical Testing of Composites*; Pendleton, R. L., Tuttle, M. E., Eds.; Springer Netherlands: Dordrecht, 1989; pp 151–164.
- (36) Malakooti, M. H.; Zhou, Z.; Spears, J. H.; Shankwitz, T. J.; Sodano, H. A. Biomimetic Nanostructured Interfaces for Hierarchical Composites. *Adv. Mater. Interfaces* **2016**, *3*, No. 1500404.
- (37) Yoshida, I.; Yokosuka, M.; Monma, D.; Ono, T.; Sakurai, M. Damping Properties of Metal-Piezoelectric Composites. *J. Alloys Compd.* **2003**, 355, 136–141.
- (38) Poquette, B. D.; Asare, T. A.; Schultz, J. P.; Brown, D. W.; Kampe, S. L. Domain Reorientation as a Damping Mechanism in Ferroelastic-Reinforced Metal Matrix Composites. *Metall. Mater. Trans. A* **2011**, *42*, 2833–2842.
- (39) Asare, T. A.; Poquette, B. D.; Schultz, J. P.; Kampe, S. L. Investigating the Vibration Damping Behavior of Barium Titanate (BaTiO₃) Ceramics for Use as a High Damping Reinforcement in Metal Matrix Composites. *J. Mater. Sci.* **2012**, 47, 2573–2582.
- (40) Wu, B. A Correction of the Half-Power Bandwidth Method for Estimating Damping. *Arch. Appl. Mech.* **2014**, *85*, 315–320.
- (41) Ewins, D. Modal Testing: Theory, Practice, and Application; Research Studies Press, 2000.
- (42) Daniel, J. I. Engineering Vibration; Prentice-Hall, Inc.: New Jersey, 2001.